Journal of Colloid and Interface Science 457 (2015) 232–242

Contents lists available at ScienceDirect

Journal of Colloid and Interface Science

journal homepage: www.elsevier.com/locate/jcis

Alkyl esters of L-ascorbic acid: Stability, surface behaviour and interaction with phospholipid monolayers

Milagro Mottola [a,b], Raquel V. Vico [b,*], Martín E. Villanueva [b], María Laura Fanani [a,*]

[a] Centro de Investigaciones en Química Biológica de Córdoba (CIQUIBIC–CONICET), Departamento de Química Biológica, Facultad de Ciencias Químicas, Universidad Nacional de Córdoba, Haya de la Torre y Medina Allende, Ciudad Universitaria, X5000HUA Córdoba, Argentina

[b] Instituto de Investigaciones en Fisicoquímica de Córdoba (INFIQC–CONICET), Departamento de Química Orgánica, Facultad de Ciencias Químicas, Universidad Nacional de Córdoba, Haya de la Torre y Medina Allende, Ciudad Universitaria, X5000HUA Córdoba, Argentina

HIGHLIGHTS

- The substitution of L-ascorbic acid with long acyl chains provides chemical stability.
- Contrary to ASC_{12} and ASC_{10}, ASC_{16} and ASC_{14} form stable Langmuir monolayers.
- ASC_n films form 2D crystalline structures growing with different azimuthal orientations.
- ASC_{16}, ASC_{14} and ASC_{12} form Gibbs monolayers and penetrate into phospholipid films.
- Only ASC_{16} forms condensed or crystalline domains in mixed films with phospholipids.

GRAPHICAL ABSTRACT

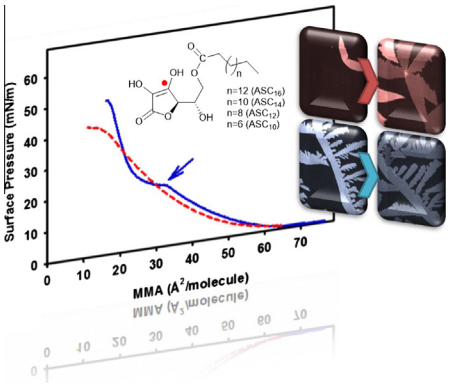

ARTICLE INFO

Article history:
Received 16 April 2015
Revised 30 June 2015
Accepted 8 July 2015
Available online 10 July 2015

Keywords:
Amphiphilic Vitamin C derivatives
Langmuir monolayers
Chiral crystalline domains
Gibbs adsorption films

ABSTRACT

L-ascorbic acid alkyl esters (ASC_n) are molecules of pharmaceutical interest for their amphiphilic nature and proposed antioxidant power. In contrast to L-ascorbic acid, ASC_n with different acyl chain lengths behaved stably upon oxidation and a tautomeric isomerization was observed. In Langmuir films, when the ascorbic ring has a negative charge, ASC_{14} and ASC_{16} form stable monolayers, contrary to ASC_{10} and ASC_{12}. ASC_{16} films showed transition from liquid-expanded (LE) to liquid-condensed phase, whereas ASC_{14} showed only an LE phase. When ASC_n are mainly neutral, ASC_{14} showed phase transition from LE to a crystalline phase, as previously reported for ASC_{16}. The two-dimensional domains displayed crystal-like shapes with anisotropic optical activity when interacting with the polarized light under Brewster angle microscopy. The compounds with the longer acyl chain (ASC_{16}, ASC_{14} and ASC_{12}) exhibited good surface activity, forming Gibbs monolayers. They also were able to penetrate into phospholipid monolayers up to

Abbreviations: ASC_n, L-ascorbic acid alkyl esters; ASC_{16}, ascorbyl palmitate; ASC_{14}, ascorbyl myristate; ASC_{12}, ascorbyl laurate; ASC_{10}, ascorbyl decanoate; POPC, 1-palmitoyl-2-oleoylphosphatidylcholine; LE, liquid-expanded phase; LC, liquid-condensed phase; C, crystalline phase; π, surface pressure; C_s^{-1}, compressibility modulus; MMA, mean molecular area; EMC, equilibrium monomer concentration; BAM, Brewster angle microscopy.

* Corresponding authors.
E-mail addresses: rvico@fcq.unc.edu.ar (R.V. Vico), lfanani@fcq.unc.edu.ar (M.L. Fanani).

http://dx.doi.org/10.1016/j.jcis.2015.07.014

Ascorbic acid tautomerization
Phospholipids mixed domains

a critical point of 45–50 mN/m. The 1-palmitoyl-2-oleoylphosphatidylcholine/ASC_n films showed LC and/or crystalline domains only for ASC_{16}. This study provides valuable evidence regarding the stability and surface properties of this drug family, and casts light into the differential interaction of these drugs with lipid membranes, which is important for understanding its differential pharmacological activity.

1. Introduction

L-Ascorbic acid (Vitamin C) is a widely used compound in pharmacological and alimentary preparations as a natural, cheap and biocompatible strong antioxidant reagent. However, its use is severely limited by its very poor solubility in non-water solvents. The substitution of ascorbic acid to produce alkanoyl-6-*O*-ascorbic acid esters (ASC_n, see Scheme 1) results in amphiphilic derivatives which have been proposed to maintain the strong antioxidant character of Vitamin C [1,2]. The presence of the acyl chain, besides improving its solubility in alcohol and non-polar solvents, provides the capacity to self-organize into micelles and coagel when suspended in water [3]. ASC_n aggregates have been proposed as drug delivery nanostructures capable of providing antioxidant protection to sensitive drugs [2] and as valuable components of phosphatidylcholine (PC)-based liposomes for drug delivery [4].

Besides its widely proclaimed antioxidant properties, the ASC_n family has been used in different pharmacological preparations per its amphiphilic nature. The addition of ASC_{12} to ocular topical preparation improves the permeation of the hydrophobic drug acetazolamide, more efficiently than ASC_{16} [5]. The same picture was observed for permeation of ibuprofen through the mouse skin [6]. Furthermore, only ASC_{12} but not ASC_{16} showed antileishmanial activity [7]. On the other hand, ASC_{16} has been proposed as the key component of a new and potent adjuvant preparation. The high immunization levels obtained were related to the induction of a local inflammatory response [8].

It is clear from the above information that the different members of ASC_n family have some differences in its effectiveness for determined pharmaceutical purposes. It was the aim of this work deepening into the understanding of the physicochemical properties of each member of this drug family since they may be determinant for their efficacy in those pharmaceutical processes, in particular those related to surface phenomena and interaction with biomembranes. As cell membranes are the first contact of lipophilic drugs with cells and often form a reservoir, the drug/membrane interaction is a fundamental condition for its pharmacological function and a potential regulatory point.

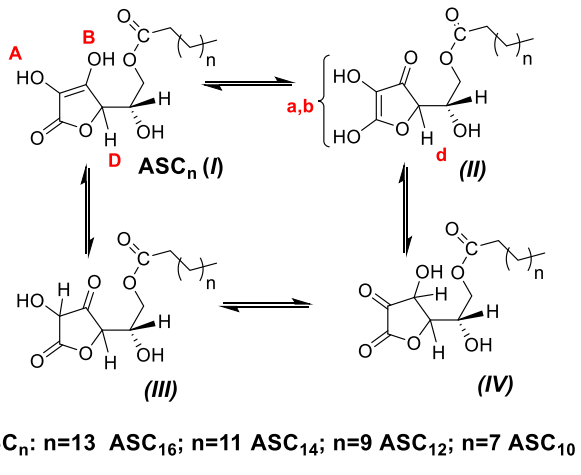

Scheme 1. Chemical structure of ASC_n (*I*) and possible tautomeric forms of ASC_n derivatives (*II*, *III*, *IV*).

The both main chemical properties of ASC_n were taken into account: their antioxidant properties and their amphiphilic character. The former has been addressed previously by different groups. To keep the antioxidant activity of Vitamin C, any derivative must preserve the –OH groups of the ascorbic ring in C_2 and C_3 [1]. It has been shown that ASC_n conserve part of the radical scavenging activity in aggregates such as micelles. For example, ASC_{10} micelles retain about half of the antioxidant performance for oxygen uptake [1], whilst ASC_{12} and ASC_{14} only retain ~40 and ~34% of the antioxidant activity [7,9] compared to unmodified L-ascorbic acid. It is well known that L-ascorbic acid is stable in solid form, but it is susceptible to oxidation when in solution. In a stability study of L-ascorbic acid carried out using NMR at different times and temperature it was shown that several aromatic (furane) and olefinic protons appears and were attributed to decomposition and/or tautomerization [10].

The amphiphilic nature of ASC_n is a dominant feature that conditions its physicochemical properties and also makes of this drug family the most appreciated for pharmaceutical purposes. The physicochemical behaviour of ASC_n has been extensively studied in drug/water systems [2,3,11], but only a few studies have investigated the surface behaviour of these amphiphiles comprising early studies on ascorbyl stearate [12–14] and more recently about ascorbyl palmitate (ASC_{16}) [15,16]. Whilst Langmuir monolayers at the air/water interface composed of ascorbyl stearate shows a completely condensed behaviour in the whole surface pressure range, the commercial product ASC_{16} forms monolayers which undergo phase transition from a liquid-expanded (LE) to a liquid-condensed (LC) or crystalline phase (C), depending on the electrostatic properties of the film conferred by ionic strength and subphase pH [16,17].

Few attempts have been made to explore the interaction and general physicochemical effect of one ASC_n family member, the commercially available ASC_{16}, when it is incorporated into biological membranes under controlled conditions [7,15,18]. We recently studied the interaction of ASC_{16} with biomembranes, using phospholipid monolayers as a model of biological membrane [15]. Our results showed a strong and complex interaction of ASC_{16} with lipid interfaces. For instance, the pH of the subphase determines both the ASC_{16} aggregation in solution and the penetration rate.

In the present work, we extend our previous research about ASC_{16} to other Vitamin C derivatives substituted by shorter length hydrocarbon chains (C14, C12 and C10, see Scheme 1) in order to evaluate the effect of acyl chain length on the surface organization of the self-assembled bidimensional aggregates as well as their interaction with biomembranes models. The non-commercial compounds ASC_{14} and ASC_{12} were synthesized in our laboratory, according to a modified version of the main procedure reported in the literature [14], and compared with the commercial ASC_{16}. Gibbs and Langmuir monolayers were studied at neutral pH where a charged surface is formed due by ionization of the C_3–OH group of the ascorbic moiety ($pK_a = 4.2$) and at acidic pH where the compounds are mainly neutral. We also explored the surface

organization of the crystalline phase formed by ASC_{14} and ASC_{16} using Brewster angle microscopy and described a birefringence effect, which reflects a tilted azimuthal orientation of the molecules in the two-dimensional structure.

Additionally, we studied ASC_n interaction with phospholipid monolayers, used as membrane model system. Phosphatidylcholines are zwitterionic lipids abundant in cell membranes and are the most studied lipid family [19]. When they contain at least one double bond in their chains represent the simplest model of biomembranes, commonly used. Palmitoyloleoylp hosphatidylcholine (POPC) is a glycerophospholipid, which is esterified with a 16:0 and an 18:1 acyl chain. It is of widespread use both in bilayers and monolayers systems since it is present as a Lα (or Liquid-disordered) phases in bilayers and a LE phase state in monolayers along all the surface pressure range, at room temperature [20]. Those liquid phases (Lα and LE) are proposed to be the major phase state found in cell membranes [19].

The present study evidenced a favourable penetration of ASC_n compounds into POPC monolayers, which in some conditions occurs with alteration of its lateral organization and formation of condensed domain. Our results cast some light into the differences of the pharmacological potential of the different members of the ASC_n family based on its surface behaviour and their interaction with lipid monolayers.

2. Experimental

2.1. Materials

Myristic acid, and (+) sodium L-ascorbate were provided by Sigma–Aldrich, Co (USA) and lauric acid by SAFC. Their purity was ascertained by ^{1}H NMR and ^{13}C NMR. Commercial 6-*O*-Palmitoyl-L-ascorbic acid (ASC_{16}) was supplied by Sigma–Aldrich, Co (USA) and exhaustively purified as described below in order to remove traces of palmitic acid detected by NMR. Sulphuric acid (J.T. Backer) used for the synthesis of ASC_{12} and ASC_{14} derivatives was 97.8%. ASC_{10} was kindly provided by Dr. Benedini, Universidad Nacional del Sur, Bahia Blanca, Argentina. 1-palmitoyl-2-oleoylphosphatidylcholine (POPC) was obtained from Avanti Polar Lipids, Inc (Alabama, USA). Solvents used in the purification of ASC_n were diethyl ether (Merck), ethyl acetate (Sintorgan) and *n*-hexane (Anedra); *n*-hexane was distilled prior to use. Silica gel 60 (0.063–0.200 mm) employed for purification was from Merck. The water was purified by a Milli-Q (Millipore, Billerica, MA) system, to yield a product with a resistivity of ~18.5 MΩ cm and a surface tension of 72.8 mN/m at 25 °C.

For TLC analysis, the samples of ASC_n were dissolved in chloroform and spotted on pre-coated silica gel G or aluminium oxide 60 F_{254}, 0.2 mm thick; different solvent mixtures of *n*-hexane/ethyl acetate or acetone/ethyl acetate were used as a mobile phase. ^{1}H NMR and ^{13}C NMR experiments were run using a Bruker Avance II 400 high-resolution spectrometer. Absorbance FT-IR spectra of ASC_n powder (mixed with KBr) were measured in a Nicolet 5XC or in a Nicolet Avatar 360 spectrophotometer.

2.2. Synthetic procedures

ASC_{12} and ASC_{14} (Scheme 1) were synthesized through a modified procedure reported in the literature [14] which involves the reaction between myristic acid or lauric acid and the primary –OH group in position 6 of L-ascorbic acid in concentrated sulphuric acid. A 100 mL sample of 97.8% sulphuric acid was placed in a two-neck round bottom flask with molecular sieve (Merck, beads 0.4 nm–2 mm, Reag. PhEur) in order to favour ASC_n formation by displacement of water from the reaction medium. A gentle stream of nitrogen was bubbled for 40 min under magnetic stirring at room temperature to remove oxygen. Then, 25 mmol of (+) sodium L-ascorbate (4.95 g) was added and completely dissolved, followed by 25 mmol of the corresponding carboxylic acid (5.31 g of lauric acid for ASC_{12} or 6.26 g of sodium myristate for ASC_{14}). The flask was kept in a nitrogen atmosphere until the reaction was completed at 45 °C. After 18 h, the mixture was slowly poured into a beaker containing ice and Milli-Q water and stirred until it reached room temperature with the formation of a white precipitate. The solution was then transferred to a separatory funnel and treated with diethyl ether several times; brine was added in order to break the emulsion. The organic phase was treated with anhydrous sodium sulphate, filtered and evaporated under vacuum.

To purify ASC_n derivatives, an amount of about 0.6 g of ASC_n was dissolved in *n*-hexane and mixed with silica gel 60 (about 1.6 g). This mixture was dried in a rotary evaporator and placed in a Büchner filter funnel with integral sintered glass discs porosity grade 3 (Pyrex). The solid was washed by rinsing with *n*-hexane (400 mL) and *n*-hexane:ethyl acetate 99:1 (400 mL) until the presence of carboxylic acid was not detected by TLC_s (TLC showed the presence of only one spot). ASC_n was extracted from the silica gel with diethyl ether, dried and stored in a flask under nitrogen atmosphere. Commercial ASC_{16} was further purified in order to remove remnant palmitic acid, which considerably affects phase transition and morphology of condensed domains in Langmuir monolayer studies. The purification process was as described above for ASC_{12} and ASC_{14}. FT-IR, ^{1}H and ^{13}C NMR and HSQC–DEPT spectra for ASC_n are shown in Figs. S1–S12 in Supporting Information file. The solutions for NMR experiments were prepared by dissolving the ASC_n samples in CCl_3D or DMSO-d6. To perform the NMR experiments along time the samples were stored at 4 °C under ambient atmosphere.

2.3. Langmuir monolayer formation of ASC_n

Compression isotherms of ASC_n Langmuir monolayers were obtained as detailed in Ref. [16]. Compression isotherms are reported as surface pressure (π) vs. mean molecular area (MMA) plots. The surface pressure was taken as shown in Eq. (1) [17]:

$$\pi = \gamma_0 - \gamma \quad (1)$$

where γ_0 and γ are the surface tension of the air/water interface in absence or presence of an amphiphile film respectively. The MMA is the total monolayer area divided by the total number of molecules at the interface. Briefly, a chloroformic solution of pure ASC_n or POPC/ASC_n mixture (1 mg/mL) was spread onto the surface of a Teflon™ trough filled with NaCl 145 mM until reaching a mean molecular area of ~100 Å^2 molecule^{-1}. After waiting 5 min for solvent evaporation and relaxation of the film at $\pi \leqslant 0.5$ mN/m, the film was compressed at a constant rate of 8 ± 1 Å^2 molecule^{-1} · min^{-1} until reaching the target surface pressure. We choose NaCl solution as the aqueous solvent for studying ASC_n behaviour to keep the system as simple as possible. The aqueous solutions used as the subphase were: saline solution at pH5 (NaCl 145 mM, whose final pH after ASC_n addition is pH = 5.0 ± 0.2) and saline solution at pH 3 (NaCl 145 mM adjusted to pH 3 with HCl, whose final pH after ASC_n addition is pH = 2.8 ± 0.2). We avoided the use of buffer as subphase solutions since the substances tested for this use showed certain surface activity by themselves. π was determined with a Pt plate using the Wilhelmy method. The equipment used was a homemade circular Langmuir balance consistent in several Teflon™ troughs of different surface areas and 0.8 cm deep (the compartment used for compression isotherms had a surface of 92 cm^2). The area accessible to the film was determined by the relative position of two Delrim™ barriers attached to a central, their

lateral movement over the trough surface was controlled and registered by an electronic unit (Monofilmetter, Mayer, Gottingen) [21]. For experiments exploring the stability of the Langmuir films a barostat was used to keep the surface pressure constant allowing the adjustment of the monolayer area. All experiments were carried out enclosed in an acrylic box under N_2 stream to prevent ASC_n oxidation.

2.4. Adsorption of ASC_n to the air/water surface and penetration into phospholipid monolayers

The adsorption of ASC_n molecules from the subphase to the bare air/water interface leads to the formation of Gibbs monolayers. Those experiments were performed by injections of typically 30–70 μL of ASC_n in ethanol (10 mg/mL) into the aqueous subphase of a Teflon trough under continuous stirring (trough volume: 15 mL). Control experiments showed no increase of π after the injection of up to 100 μL of ethanol into the subphase. The final subphase concentration of ASC_n was chosen above the monomer concentration in equilibrium with the supramolecular aggregates for each compound (see details in Section 3 and Fig. S19 in Supplementary material and Ref. [15]): 18, 20 and 50 μM for ASC_{16}, ASC_{14}, and ASC_{12}, respectively, unless specified. The changes in π at constant area were registered as a function of time, whilst a Gibbs monolayer was established at the air/water surface. After adsorption of the ASC_n amphiphiles to the surface, the subphase concentration may diminish in less than 4%. For penetration experiments, a phospholipid monolayer composed by pure POPC was formed by deposition of a chloroformic solution of the lipid at the air/water interface until achieving the target π previous to the injection of ASC_n into the subphase. All experiments were performed at 23 ± 2 °C and carried out enclosed in an acrylic box under N_2 stream to prevent ASC_n oxidation.

2.5. Compressibility analysis of Langmuir and Gibbs monolayers

In order to analyse the elastic behaviour of the films, the compressibility modulus (C_s^{-1}) was calculated as follows [17]:

$$C_s^{-1} = -A\left(\frac{d\pi}{dA}\right)_T \quad (2)$$

where A represents the total monolayer area. For Langmuir isotherms, the $d\pi/dA$ data was obtained from regular compression experiments and for Gibbs monolayers from the $d\pi/dA$ plot slope obtained upon compression of equilibrated adsorbed monolayers (typically 30 min after injection of ASC_n into the subphase).

2.6. Brewster angle visualization

Langmuir monolayers were prepared as described above, using a KSV Microtrough apparatus (KSV NIMA-Biolin Scientific AB, Västra Frölunda Suecia). The Langmuir equipment was mounted on the stage of a Nanofilm EP3 Imaging Ellipsometer (Accurion, Goettingen, Germany), which was used in the Brewster Angle Microscopy (BAM) mode. Minimum reflection was set with a polarized laser (532λ) incident on the bare aqueous surface at the experimentally calibrated Brewster angle (~53.1°). After monolayer formation and during compression, the reflected light was collected through a 20× objective and an analyser-polarized lens to a CCD camera.

The grey level at each pixel of the BAM images can be converted to reflectivity values applying calibration factors, set for each experiment. For 2D isotropic films, the reflectivity obtained from BAM measurements is related to the square of the film thickness and to the refractive index of the film, and is polarized in the same direction as the incident beam [22]. In films which show 2D anisotropy and the symmetry axis does not coincide with the incidence plane, the reflected light may show a change in the polarization plane due mainly to the refractive index having a different value in the direction of the hydrocarbon chains and in orthogonal direction [22,23]. Therefore, in some experiments we set the analyser polarized −45° or +45° from the plane of the incident beam to study these birefringence effects. For a better visualization, in Figs. 2, 3 and 5, the lower 0–100 grey level range (from the 0 to 255 original scale) was selected using the free software ImageJ 1.43u (NIH, USA) in order to maintain the ratio of grey level to film thickness. This experimental set-up does not allow to work under a N_2 enriched environment. However, as it will be discussed latter, the absence of a N_2 atmosphere does not significantly affect Langmuir film properties.

3. Results and discussion

3.1. Stability of ASC_n derivatives in solid state and solution

Recently, we studied the properties of ASC_{16} in 2D self-organized systems at the air/water interface [16]. Even when all monolayer experiments were carefully performed under a nitrogen atmosphere (in order to prevent oxidation) some interesting features related to subtle changes in phase states, phase transitions and also at the topological level were observed. Those changes may be attributed to impurities or to the presence/appearance of small amounts of other chemical species (such as oxidized or tautomeric products acting as impurities) in the monolayers. The antioxidant performance of ASC_n derivatives (which imply its oxidation) is in general low compared to that of L-ascorbic acid [7,9]. This trend could be attributed to a stabilization effect caused by the presence of the acyl chain or to a diminishment in the effective concentration of the active compound due to chemical change. Considering this, the stability of ASC_n derivatives was carefully studied in the present work, especially because of the properties of 2D-organized systems as well as its interactions with model biomembrane systems are highly dependent on the composition and chemical identification of their constituents [15,16]. Thus, special attention was paid to the stability to oxidation and tautomerization of the ASC_n compounds in solid state, solvent solution and when organized at the air/water interface.

Stability of solids ASC_n (mixed with KBr) was studied along time by FT-IR spectroscopy. The IR spectra showed characteristic absorptions bands that were unmodified along two weeks under ambient conditions (see Figs. S1–S3 in Supplementary Material). Similar behaviour regarding solid state stability was previously reported for L-ascorbic acid [10]. To compare the stability of ASC_n in solution with that of L-ascorbic acid (previously studied in the polar aprotic solvent DMSO) [10], we perform a stability study by ^1H and ^{13}C NMR as a function of time. Considering that DMSO is a solvent already used for biomedical purposes, the knowledge of the stability of ASC_n derivatives in DMSO is of interest for pharmaceutical and biomedical applications [24]. On the other hand, since our studies regarding surface organization in monolayers were performed by spreading ASC_n stock solutions mainly composed by chloroform at the air/water interface, it was of our concern also evaluate the stability in this solvent. ASC_n appear to be stable in both CCl_3D and DMSO-d6 solvents (see S4–S14), in contrast with their precursor compound L-ascorbic acid [10].

The NMR study performed in chloroform was carried out for ASC_{16}. A 40 mM solution of ASC_{16} was analysed using ^1H, ^{13}C, and HSQC–DEPT NMR experiments (Figs. S4–S6) along a period of 30 days. From the NMR spectra it is clearly evident that no changes occur in ASC_{16} structure in chloroform during this period of time. The stability study performed in DMSO solutions was carried out

for ASC_{16}, ASC_{14}, and ASC_{12} (in concentration of ~5 mM). All of them behaved similarly within the period of time studied (7 days), without the appearance of olefinic or aromatic signals as occurs with unmodified Vitamin C [10]. Interestingly, the NMR spectra allowed us to detect the presence of small amount of ASC_n tautomer/s in DMSO solutions. The possible tautomeric species are shown in Scheme 1 [25]. Although no attempts were made to identify if one or more tautomer/s were present, it seems to be plausible that a major contribution is given by structure *II* shown in Scheme 1, but we cannot discard the presence of compounds *III*, *IV* or their mixture as proposed by Berger for Vitamin C [25].

NMR spectra of ASC_n (5 mM, DMSO-d6) were acquired right after of solution preparation and after 7 days. The spectra displayed in Fig. S13 for ASC_{16}, acquired at time zero, shows the hydroxyl groups of the ascorbic acid ring (named A–C) and the proton named D. After a week new signals are observed (named a, b, d in Fig. S13) that can be attributed to a tautomeric form. Upon the addition of deuterium dioxide (D_2O) the signal corresponding to −OH groups disappear, as expected. The same features were present for ASC_{14} (Fig. S14) and ASC_{12} (spectra not shown). In order to confirm the presence of the tautomer/s HSQC–DEPT experiments of a 50 mM solution of ASC_{16} were performed at time zero and after 8 days. These experiments allowed us to confirm the presence of these tautomeric species, as shown in Figs. S15 and S16.

The amount of tautomer/s in ASC_n was roughly estimated by integrating ^1H NMR signals corresponding to protons D and d (see structures in Scheme 1 and Figs. S13–S14). The NMR results show that the quantity of tautomer/s increased with time, and depend on the alkyl chain length, as summarized in Table S1 (see Supporting Information). The fact that the tautomeric equilibria in ASC_n derivatives was reached slowly, may be attributed to the formation of aggregates in the organic solvent as was reported before for other amphiphiles [26–28]. The presence of this tautomeric equilibria, and probably the establishment of a hydrogen bonding network between the ascorbic acid moieties in the self-organized systems may account for the decrease in the antioxidant activity observed for ASC_n [1,9]. These reversible molecular features also could explain the changes in phase states, the phase transitions and topography observed in the monolayers experiments, as discussed latter.

3.2. Langmuir monolayers of ASC_n

When a chloroform solution of ASC_{16} is spread onto the air/NaCl solution interface a Langmuir monolayer is established. Even when the monolayer, as spread, does not represent the state of absolutely stable equilibrium, meaningful experiments can be performed on it [17]. When formed over a saline solution at near-neutral subphase pH, the ASC_{16} films have a significant amount of acidic dissociation (30–40% of the ASC_{16} molecules are negatively charged [16]). These partially charged films show a liquid-expanded (LE) to liquid-condensed (LC) phase transition at a surface pressure (π) of ~20 mN/m (Fig. 1A), as previously reported [16]. Substituting the ASC_n compound with a two methylene shorter acyl chain, ASC_{14}, results in compression isotherms almost superimposable with that of ASC_{16} at low π values, but it lacks the characteristic phase transition of ASC_{16} films, showing a smooth compression curve (Fig. 1A). This behaviour is expected, since reducing the length of the acyl chain may diminish the intermolecular Van der Waals interactions that are important for the formation of condensed phases. This effect leads to a shift of the phase transition to higher π, as was observed for several lipid families [29,30]. ASC_{14} films also showed a lower collapse pressure, a parameter which represents the highest π value reached until the monolayer enters equilibrium with 3D structures growing underneath the surface plane. On the other hand, neither ASC_{12} nor ASC_{10} compounds showed any increase in π upon compression after spreading at the interface (not shown). This may be a consequence of the fact that short acyl chains provide weaker intermolecular (Van der Waals) interactions at the surface film, allowing a rapid equilibrium with the monomeric form at the bulk subphase.

All Langmuir monolayers (also called insoluble monolayers) represent metastable systems. If there is a sufficiently significant energy barrier, the rate of approach to absolutely stable equilibrium is very small, and the system can remain in such metastable state for an extended period of time [17]. For ASC_{16} and ASC_{14} films, the stability at the surface was studied by assessing the percentage loss rate of the monolayer area when kept at a constant surface pressure (Fig. S17) and also by performing consecutive compression-expansion cycles (Fig. S18A and B). The loss of molecules at the interface at constant π and along consecutive cycles is low for the ASC_{16} film but increases several times for ASC_{14} monolayers, thus evidencing a lower stability for the latter at the interface (see Table 1). As a comparative point, a monolayer composed of stearic acid, a lipid molecule which forms insoluble monolayers, suffers a loss of ~10% of the monolayer area 30 min after spreading [17], whilst ASC_{16} lost only ~9% (Fig. S17). The stability of ASC_n Langmuir films may be also related to the packing parameters (Pc) [31] for those compounds. This parameter relates the cross-sectional area of the molecules with their estimated volume and length, and provides a rough interpretation of the general geometry of the amphiphile. For ASC_{16} and ASC_{14} a Pc ~ 1 was estimated [3], which evidences a near cylindrical geometry. This property may provide good stability in planar bidimensional aggregates, as in the case of Langmuir monolayers. In contrast, a Pc < 0.6 was estimated for ASC_{12} and ASC_{10} [3], which suggests a conical geometry and a poor ability to closely pack in a planar membrane.

When formed above a saline subphase adjusted at pH 3, Langmuir monolayers of ASC_n are formed mainly by neutral molecules [16], which can laterally aggregate in more condensed structures. For ASC_{16}, this induces a lowering of the π at which the LE–LC phase transition begins (compare Fig. 1A and B), and the condensed phase also shows characteristics of a solid or crystalline (C) more than a LC phase [16]. In this pH condition, ASC_{14} films, which behave as a LE phase in the whole π range at neutral bulk pH, showed a phase transition from a LE to a LC (or C) phase at ~30 mN/m (Fig. 1B). This effect may be a consequence of stronger intermolecular interactions, likely due to a more dense packing between the neutral ASC_n compared to the negative-charged molecules. Furthermore, Langmuir monolayers of ASC_{14} and ASC_{16} at acidic pH appear to be even more stable than at neutral pH, since the monolayer area loss is smaller at constant pressure and after compression-decompression cycles (see Figs. S17 and S18 and Table 1). On the other hand, ASC_{12} form only unstable Langmuir monolayers, whose compression curves strongly depend on the compression rate (not shown).

We have also observed that, in films showing phase transition, the compression curves show a very sharp change of slope at the transition pressure in the first compression cycle and a smoother (or less cooperative) behaviour in the second compression curve (see Fig. S18A, C and D). This suggests the presence of other species acting as impurities that appear with time in the ASC_n films. Such species can only be a consequence of a chemical change occurring at the interface; both tautomerization and oxidation of ASC_n may be responsible for this behaviour.

To explore whether oxidation plays an important role in changing the film's properties over time, we performed the Langmuir experiments in the presence and absence of N_2 atmosphere. No difference was observed in the compression curves of ASC_n monolayers in either condition, which suggests that tautomerization rather than oxidation may be taking place on ASC_n films in a detectable way after ~30 min of film formation. This oxygen independent

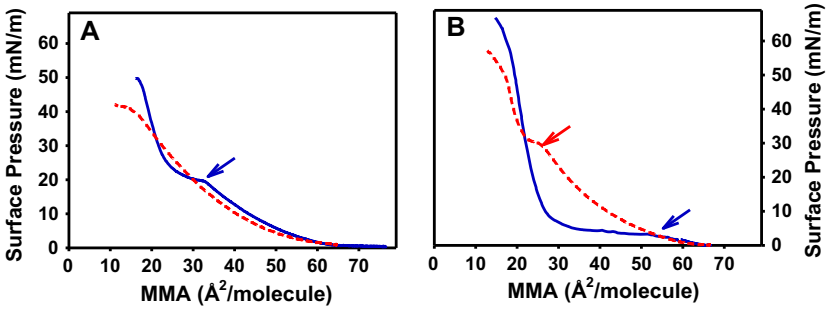

Fig. 1. Isothermal compression of Langmuir monolayers of ASC_{16} (blue, full lines) and ASC_{14} (red, dashed lines) at near- neutral (A) and acidic pH (B). The arrows indicate the beginning of the phase transition upon compression. In all cases, representative experiments are shown that vary by not more than 2 mN/m from its replica. (For interpretation of the references to colour in this figure legend, the reader is referred to the web version of this article.)

Table 1
Molecular, rheological and thermodynamic parameters of ASC_n Langmuir films at 30 mN/m.

ASC_n species*	MMA (Å²/molecule)	C_s^{-1} (mN/m)[a]	Phase state	Monolayer area loss rate at 30 mN/m (%/min)[b]	Monolayer area loss after second compression (%)	ΔG_{comp} (cal/mol)[c]	ΔG^{hys} (cal/mol)[d]
At neutral pH							
ASC_{16}	23 ± 1	66 ± 3	LC	0.43 ± 0.04	1.9 ± 0.8	370 ± 4	−99 ± 8
ASC_{14}	24 ± 1	33 ± 2	LE	5.49 ± 0.19	9.4 ± 0.8	317 ± 9	−99 ± 6
At acidic pH							
ASC_{16}	23 ± 1	163 ± 15	C	1.10 ± 0.01	0.7 ± 0.3	123 ± 4	−76 ± 3
ASC_{14}	25 ± 1	18 ± 1**	LE-C	2.55 ± 0.05	1.8 ± 0.9	296 ± 2	−77 ± 2

Figures correspond to average values and error to SEM of at least two independent experiments.
* ASC_{12} and ASC_{10} do not form stable Langmuir monolayers, either at neutral or at acidic pH.
** ASC_{14} at acidic pH and 40 mN/n, when it is in full crystalline (C) state, shows C_s^{-1} values of 82 ± 3 mN/m.
[a] Calculated after Eq. (2).
[b] Calculated for the slope of curves shown in Fig. S17 during the first 5 min.
[c] Integrating compression isotherms from 1 to 30 mN/m after Eq. (S1).
[d] Calculated after Eq. (S2).

effect is in agreement with the NMR data of DMSO solutions that suggest stability of ASC_n against oxidation (see Figs. S7–S16).

The compression–expansion cycles experiments also allowed us to explore the occurrence of a hysteresis effect on ASC_n films under both pH conditions studied. The energy given to the system upon film compression (ΔG_{comp}, reflected by the area under the π vs. MMA curve, see Section 2 in Supporting Information and Ref. [32]) was not completely restored after expansion of the film (Table 1). This effect indicated that the system retained a certain amount of energy that was stored as part of the intermolecular interaction of the film components and was not reversibly given to the system (see Eqs. (S1) and (S2)). Such phenomena are not often found in lipid films in the LE state, but have been reported for protein or lipid–protein and lipid–nanoparticles films [33–35] and for synthetic amphiphilic molecules able to establish intermolecular H-bonds [36,37].

The ASC_n films studied at different pH require different amounts of energy to be compressed up to 30 mN/m, as shown in Table 1. However, as a general trend, the films formed by ASC_n at acidic pH showed lower ΔG_{comp} than those formed at neutral pH. This may reflect higher intermolecular interaction energy between the neutral amphiphilic molecules than between charged ones, which more efficiently counteract the loss of entropy upon compression. Besides the above differences, the amount of energy stored after expansion (ΔG^{hys}) remains almost identical for ASC_{16} and ASC_{14} at both pH. This may reveal the intermolecular interaction between the ascorbic rings through hydrogen bonding, which appears identical for both ASC_n films analysed.

3.3. Surface texture of ASC_n films at acidic subphase pH

In a previous study, we explored the bidimensional structure of condensed ASC_{16} aggregates by BAM [16]. At near-neutral or higher pH, ASC_{16} films form LC domains that have a pattern of small domains with highly undulated borders and a uniform grey level. In contrast, at low pH (or low ionic strength), the large domains formed in the LE-condensed coexistence region show sharp edges that suggest a crystalline nature (Fig. 2A and B and [16]). The crystalline domains formed have a preferential growth at certain angles to one of the borders. It is worth noting that, when the film is compressed at a slow rate, a different type of 2D structure appears on the surface, growing from the borders of previously formed domains or as independent rounded domains (arrows in Fig. 2A). This can be attributed to the possible formation of other species over time, such as the tautomeric products mentioned above.

When the films were compressed at a fourfold faster rate, these structures were not observed and the texture of the films was more ramified and complex than the slowly compressed films (Fig. 2B). This suggests that the growth of the domains occurs in a far-from-equilibrium situation, where the incorporation of new molecules in the more favourable lateral face of the solid domain is counteracted by the line tension. The latter induces a lowering of the domain perimeter and rounding of its structures, a phenomenon which has been reported previously for lipid films [23,38,39].

The ASC_{14} films at pH 3 and in the slow compression rate show the formation of domains in a crystalline structure with preferential growth towards one of the axes of the domains, which strongly resembles that of ASC_{16} films. However, these structures appear more elongated than in the case of ASC_{16} (compare Fig. 2A and C). A fourfold faster compression induces the formation of feather-like structures growing asymmetrically from both sides of a curved main axis (Fig. 2D), which rapidly cover the surface of the film and undergo a smoothing of their borders when compression stops (not shown).

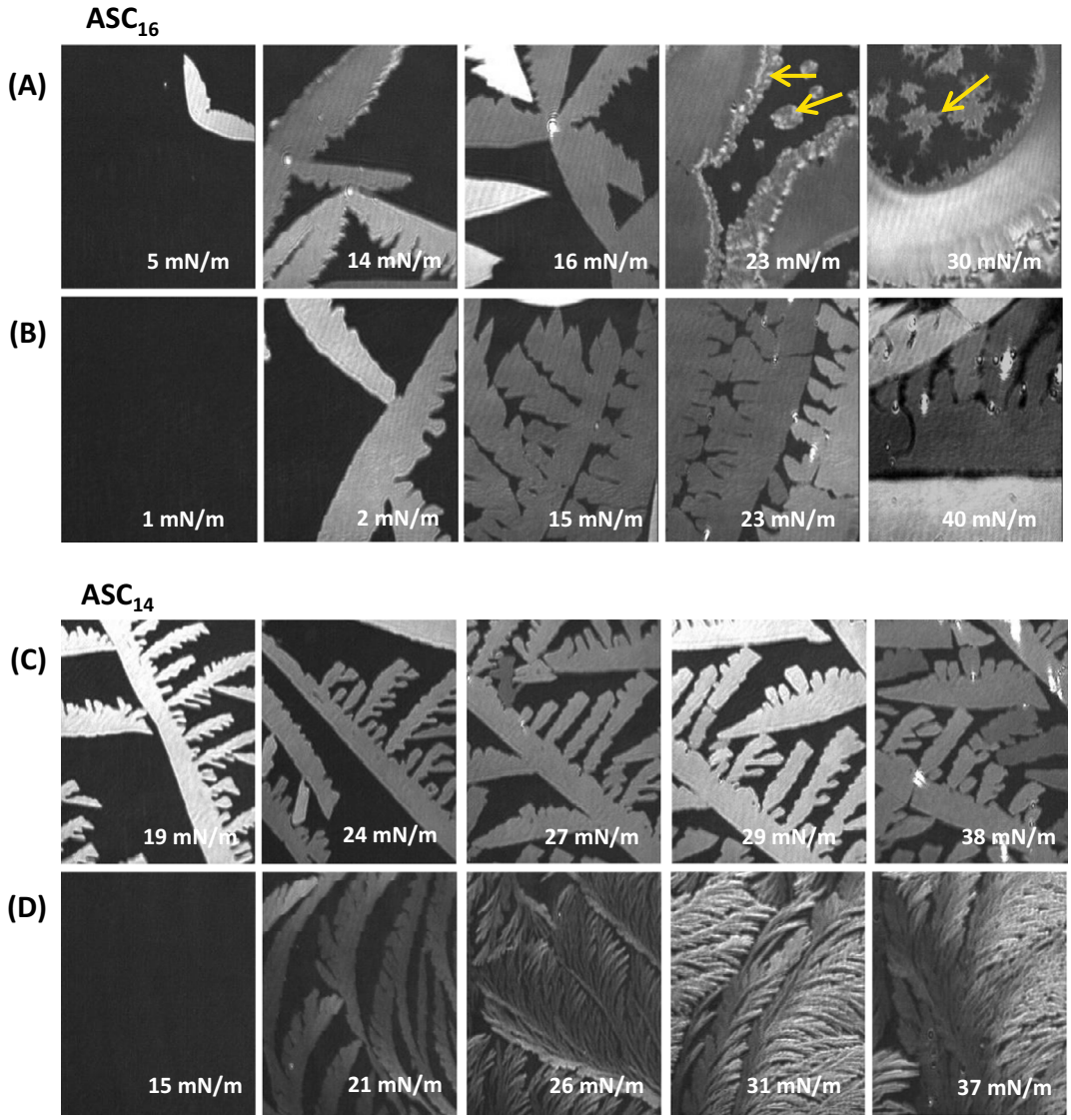

Fig. 2. Brewster angle microscopy visualization of ASC_{16} and ASC_{14} films at pH3. The yellow arrows highlight the occurrence of the aggregation of "tautomeric or oxidized" forms of ASC_n. The compression rates were 0.5 (A and C) or 2 (B and D) $Å^2$ molecule^{-1} min^{-1}. Representative images were taken from two independent experiments. Image size: 200 × 250 μm. (For interpretation of the references to colour in this figure legend, the reader is referred to the web version of this article.)

Asymmetry in the crystalline structure of phospholipid domains has been earlier related to the occurrence of a chiral carbon in the amphiphile structure [23,40] and the characteristic curved structure of dipalmitoylphosphatidlcholine (DPPC) condensed domains has also been attributed to chiral interactions [41]. The chiral structure offers a lateral surface which has comparatively more favourable interaction energy with its neighbour, and thus a preferential orientation is propagated in this direction. In the case of DPPC, the chirality is paired with the large size of the headgroup in relation to the cross-section of the aliphatic chains; this leads to a spontaneous curvature of the domain borders within the plane of the monolayer [41].

The chiral carbons of the L-ascorbic acid ring may account for the asymmetric interaction and growth of the domains. Also, the large headgroup (the ascorbic ring) compared to the cross-section of the hydrophobic portion (a single acyl chain) of ASC_n highlights some parallelisms with the phospholipid systems that may also account for the curved structure of the ASC_n lateral aggregates (in particular the ASC_{14} domains).

A general inspection of Fig. 2 shows that the crystalline domains have different brightness levels in different image regions by BAM microscopy. For an isotropic medium in the plane of the interface, the reflected light has the same polarization plane as the incident light beam. This is not the case when the sample is optically anisotropic and their symmetry axes are not in the plane of incidence [22,23]. This generates a birefringence phenomenon where the refractive index has a different value in the direction of the hydrocarbon chains and in the orthogonal direction.

Crystalline domains of ASC_{16} and ASC_{14} showed this birefringence phenomenon. This is evident since some regions of these domains (or some domains in comparison with their neighbours) appeared of different brightness. This suggests that their molecular axes were tilted from the normal to the interface. Thus, different domains showed different local orientations of the tilt azimuth, since they could form and rotate (at early stages of the compression process) independently from their neighbour domains.

To support this hypothesis, we evaluated the brightness level of neighbouring domains at different orientations of the A-polarizer (after the sample-light interaction). The samples interact with the normally polarized light, altering the resultant polarization plane, so that the reflected light becomes a function of the angle α formed by the A-polarizer and the normal plane. BAM images

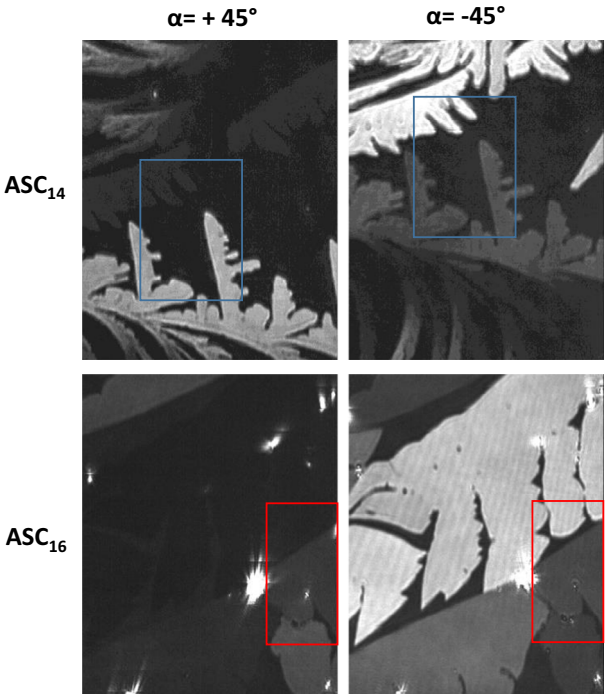

Fig. 3. BAM images for ASC_{16} and ASC_{14} Langmuir films at pH3 when the A-polarizer is set to $\alpha = +45°$ and $\alpha = -45°$. The frames highlight the same monolayer area at different polarizer positions. Representative images were taken from two independent experiments. Image size: 200 × 250 μm.

of ASC_{14} and ASC_{16} monolayers (2–4 mN/m above the corresponding transition pressure) were taken by setting the angle α of the A-polarizer to +45° and −45° (Fig. 3). The images show a change in the brightness of neighbouring domains with different in-plane orientation for both ASC_n.

The tilted orientation of the ASC_n molecules in the crystalline domains (C phase) may strongly contribute to intermolecular condensation energy. From Langmuir monolayers, we found that the compression of ASC_n monolayers at acidic pH (LE–C phase transition) required less energy than at neutral pH (LE–LC phase transition, see Table 1). Since the ASC_n amphiphiles are dipolar molecules [16], and the normal dipole components contribute only weakly to the dipolar molecular interaction, the tilted azimuth of this molecular arrangement may induce an in-plane dipolar component that strengthens the intermolecular interactions. This effect may further contribute to the asymmetry of the mesoscopic-range (μm size) structures, as they form higher multipoles with neighbouring molecules [41].

3.4. Gibbs monolayers of ASC_n

When a concentrated solution of ASC_n was dissolved in the bulk of an aqueous solution, the adsorption of these amphiphilic molecules to the air/water interface resulted in a Gibbs monolayer, evidenced by a decrease in the surface tension (or an increase of π) (Fig. 4A and B). The surface pressure reached at equilibrium (π_{eq}) increase with the subphase amphiphilic concentration when it falls below a critical monomer concentration (called equilibrium monomer concentration, EMC). Above this EMC, the ASC_n molecules form supramolecular structures such as micelles or lamellas in

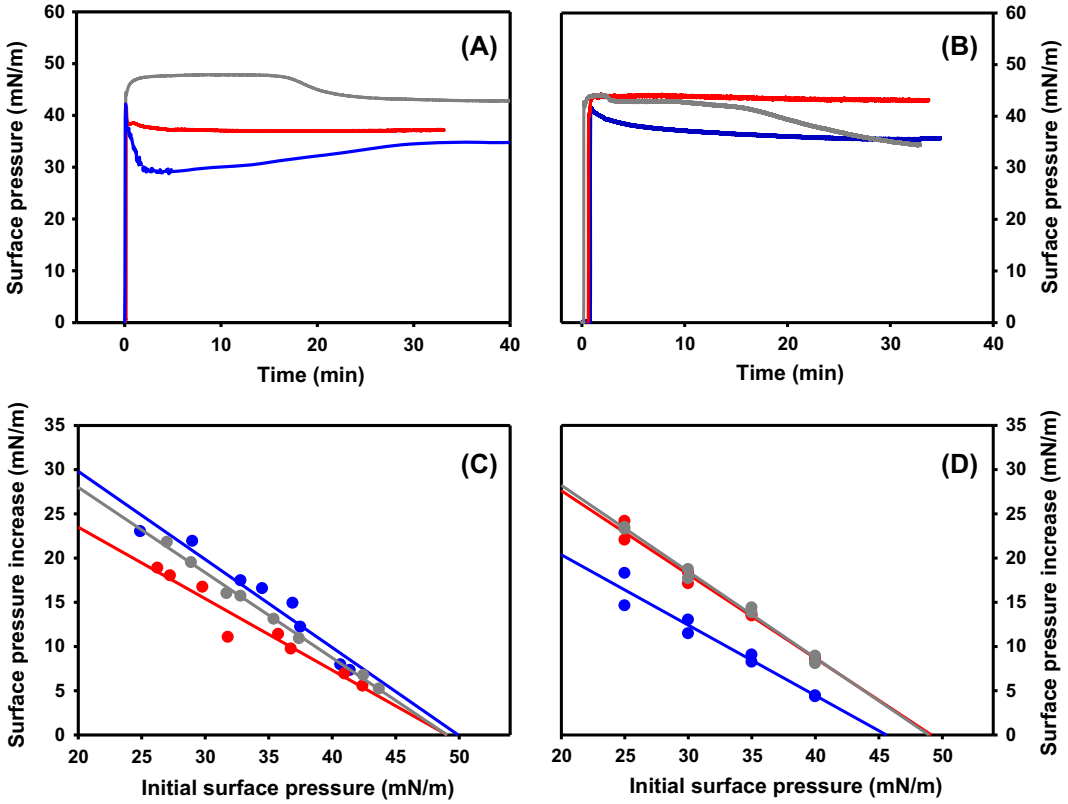

Fig. 4. Time curves for Gibbs monolayers formation (A, B) and phospholipid monolayer penetration cut off curves (C, D) by ASC_n at near neutral (A, C) or acidic pH (B, D). (A, B) The films were formed after injection of ASC_n into the subphase. In all cases, representative experiments are shown that vary by not more than 2 mN/m from its replica. (C, D) Cut off curves for penetration of ASC_n into pre-formed POPC films at different initial surface pressures. The final subphase ASC_n concentration is above the equilibrium monomer concentration in all cases: 50, 20 and 18 μM for ASC_{12}, ASC_{14}, and ASC_{16}, respectively. Colour codes are: ASC_{12} (grey), ASC_{14} (red) and ASC_{16} (blue). (For interpretation of the references to colour in this figure legend, the reader is referred to the web version of this article.)

Table 2
Gibbs monolayers of ASC_n and its penetration into phospholipids monolayers.

ASCn species*	At bare air/water interface						Into pre-formed POPC monolayer	
	π_{eq} (mN/m)	EMC (μM)	C_s^{-1} (mN/m)[a]	Estimated MMA (Å^2/molecule)[b]	Estimated C_s^{-1} (mN/m)[b]	Estimated phase state[b]	Penetration π_{eq} (mN/m)[c]	Cut off (mN/m)
At neutral pH								
ASC_{16}	34 ± 1	8 ± 2**	220 ± 9	22 ± 1	78 ± 6	LC	50 ± 1	50 ± 6
ASC_{14}	37 ± 1	9 ± 3	26 ± 1	20 ± 1	29 ± 1	LE	46 ± 2	49 ± 6
ASC_{12}	40 ± 2	33 ± 3	29 ± 2	no LM	no LM	no LM	48.5 ± 0.4	49 ± 2
At acidic pH								
ASC_{16}	35 ± 1	8 ± 1**	145 ± 7	21 ± 1	170 ± 12	C	43 ± 1	46 ± 5
ASC_{14}	35 ± 1	nd	94 ± 7	20 ± 1	64 ± 1	C	48 ± 1	49 ± 3
ASC_{12}	39 ± 1	nd	62 ± 3	no LM	no LM	no LM	48.5 ± 0.5	49 ± 2

Figures correspond to average values and SEM of at least two independent experiments. "nd" stands for not determined and "no LM" stands for not forming Langmuir monolayers.
* ASC_{10} did not form Gibbs monolayers neither were able to penetrate into pre-formed lipid monolayers.
** Extracted from [15].
[a] Measured upon compression of Gibbs monolayers after equilibration.
[b] Estimated from Langmuir monolayer isotherms under the assumption that Gibbs monolayers keep the molecular and thermodynamic characteristics of Langmuir monolayers [43].
[c] Measured at an initial surface pressure of the POPC monolayer of ~30 mN/m.

equilibrium with the monomeric form and the monolayer film (see Section 3, in Supplementary Material). Then, in contrast to Langmuir monolayers, Gibbs monolayers reflect the equilibrium between the bulk form of the amphiphile and the organized film at the interface.

As previously reported, the ASC_{16} adsorption curve shows a biphasic mode with a transitory peak due to the establishment of a double layer of ions underneath the negatively charged film, which results in a drop of the surface pH followed by a slow rise to equilibrium values (see Fig. 4A) [15]. The presence of an initial peak was also observed for the adsorption of amiodarone (cationic amphiphilic drug) to the air/water interface [42], suggesting a general behaviour for the adsorption of charged amphiphiles. Fig. 4 also shows the adsorption curves for ASC_{14} and ASC_{12} both at neutral and acidic pH. All the ASC_n films induce a significant increase in π to the 34–40 mN/m range meaning that they can lower the surface tension from 72 to 32–37 mN/m (see Table 2). On the other hand, the shortest compound tested, ASC_{10}, does not show any increase in π when injected into the subphase up to millimolar concentrations (not shown).

The variation of π_{eq} (or equilibrium surface pressure) upon an increase in bulk ASC_n concentration gives information about the equilibrium between the subphase aggregates and monomers. It was reported that at 30 °C and in pure water, ASC_{12} and ASC_{14} show a critical micellar concentration of ~100 and ~10 μM respectively, whilst ASC_{16} form not micelles but coagels [3]. Taking into account that the presence of salt in the medium strongly influences the ionization of the ASC_n molecules at the aggregate surface/water interface [16], we previously studied the subphase aggregation of ASC_{16} in high ionic strength conditions and reported the occurrence of a structure which diffracts X-rays according to a lamellar organization with an EMC of 8 ± 2 μM [15]. In the present work and for shorter ASC_n, we observed a break in the π_{eq} vs. ASC_n concentration plot (Fig. S19), which evidences an EMC of the same magnitude as ASC_{16} for ASC_{14} and threefold higher for ASC_{12} (see Table 2), which is as expected for a more hydrophilic compound. These values are in a similar concentration range to that previously reported in water solution [3].

We further studied the rheological properties of the Gibbs monolayers by determining the compressibility modulus (C_s^{-1}) of the film by compressing the adsorbed film after reaching the subphase–surface equilibrium (Table 2). Similar to Langmuir monolayers, this parameter reflects the response in π to compression of the film and is expected to be low for fluid monolayers and higher for condensed films. For different amphiphilic systems, strong correlations have been found between the properties of Langmuir and Gibbs monolayers [43], and thus a comparison may give valid information for both systems. Although the analysis values of C_s^{-1} for Gibbs and Langmuir monolayers from Table 2 do not show a close match, some general tendencies may be found. The films indicated as being in LC or C state in Langmuir monolayers also show the highest C_s^{-1} values for Gibbs monolayers, and therefore a condensed character may be attributed to them. In addition, the analysis of Gibbs monolayers enabled us to assign an LE character to the ASC_{12} films, which do not form stable Langmuir films. It is worth noticing that for the Gibbs monolayers indicated as being in a condensed state the π_{eq} reached were lower than for the LE films (see Table 2). This effect may reflect the dynamic process of incorporation of an amphiphile molecule into an established film, which may require the lateral displacement of film components to place a new one. The energy for this displacement must be related to the rheological properties of the film.

Finally, we estimated the mean area occupied by a molecule in Gibbs monolayers by assuming a similar lateral organization as in Langmuir monolayers (at similar π). Table 2 shows that such values of MMA are in the 20–22 Å^2/molecule range. This coincides with the cross section of 21 Å^2/molecule reported for ASC_{16} and ASC_{14} estimated from the application of the Gibbs equation for adsorbed monolayers at the air/water interface [3]. Considering that the cross section of a single acyl chain occupies 18 Å^2/molecule [17], these values suggest a close packing of ASC_n molecules in Gibbs monolayers.

3.5. Penetration of ASC_n into phospholipid monolayers and properties of mixed films

The interaction of ASC_n with lipid membranes was studied using phospholipid monolayers as biomembrane model system. When a concentrated solution of ASC_n is injected into the subphase of a pre-formed lipid monolayer, the further increase in π of the films evidences the penetration of the amphiphile into the lipid membrane (see Fig. S20 for representative curves).

Similar to that previously reported for ASC_{16} [15], ASC_{14} and ASC_{12} (but not ASC_{10}) penetrate into phospholipid monolayers initially at 30 mN/m until reach a π_{eq}, which is 8–16 mN/m higher than when are adsorbed to bare air/water surface (Table 2).

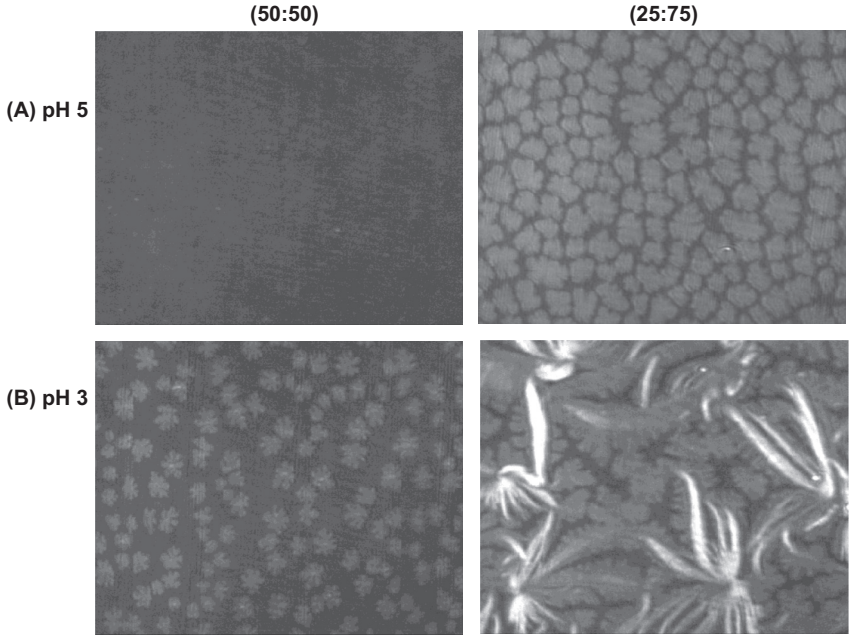

Fig. 5. BAM images for mixed monolayer containing POPC/ASC_{16} 50:50 M ratio (left panel) or 25:75 M ratio (right panel) at ~40 mN/m. The subphase was at neutral (A) or acidic pH (B). The mixed monolayers proved to be stable enough (it was not detected a large desorption of molecules, which would produce a loss of the molecular area) to be manipulated under the BAM equipment for a lapse of ~30 min. Representative images were taken from two independent experiments. Image size: 250 × 200 μm.

Penetration experiments of ASC_n into POPC monolayers were performed at different initial values of π. The further increase in π after ASC_n addition depended on the initial π, as shown in Fig. 4C and D, determining the extrapolated maximum π at which each ASC_n would be able to penetrate (cut off point). These values are in the range of 45–50 mN/m for all cases studied (Table 2). This agree with the pressure range found when interacting with the mimetic membrane of leishmania [7]. It is worth noting that these cut off values are far higher than the average surface pressure assigned to bilayers membranes (30–35 mN/m, see [44,45]), therefore this suggest that the ASC_n family is also able to penetrate into lipid bilayers.

Since the penetration process involves enrichment of the lipid film with ASC_n molecules, we further studied the properties of POPC/ASC_n binary Langmuir films at a surface pressure comparable to the reached by penetration experiments (~40 mN/m). Both POPC/ASC_{12} and POPC/ASC_{14} films at neutral or acidic pH and in the (1:1) or (1:3) mole ratio showed a single phase, which behaves as a LE phase when visualized by BAM (not shown but similar to Fig. 5A, left panel). However, ASC_{16} showed the presence of LC domains with homogeneous grey levels and undulated borders both at neutral pH containing 75 mol% and at acidic pH at 50 or 75 mol% of ASC_{16} (Fig. 5). At high content of ASC_{16} and in acidic pH it is also observed the occurrence of a third phase with long curved birefringent domains (Fig. 5B, right panel), which resemble the C phase structure formed by pure ASC_{16} in similar conditions.

4. Conclusions

Our studies revealed that, in contrast to L-ascorbic acid, the alkyl ester derivatives (ASC_n) behave stable towards oxidation in all the organization states studied. In agreement with previous studies [1] this suggests that its antioxidant activity might be diminished in comparison with L-ascorbic acid. In addition, a tautomeric equilibrium was observed, showing a faster dynamic when the acyl chain is shorter. In summary, the substitution of L-ascorbic acid with a long acyl chain provides a chemical stability to compound proportional to the length of the substituent.

The shortening of the acyl chain in ASC_n also favours the formation of LE films when organized at the air/water interface and, for very short acylated compounds (ASC_{12} and ASC_{10}), Langmuir films were no longer stable. At low pH, the C_3-OH of the ascorbic ring of ASC_n is protonated, producing mainly neutral molecules that stabilize the condensed phase of ASC_{16} and ASC_{14}, which appear as crystalline bidimensional structures by BAM, showing an asymmetric growth of the domains in an ordered tilted configuration, probably influenced by the presence of two chiral carbons in the ascorbic moiety structure.

The ASC_n members with acyl chains $\geqslant$ 12 carbons showed high surface activity and are able to form Gibbs monolayers with an equilibrium pressure in the same range than the estimated for lipid bilayers and for cell membranes [44,45]. Those adsorbed films reach relatively higher surface pressures forming loosely packed films (LE phases), and those showing a more solid-like rheology present slightly lower pressures. This may reflect the importance of surface rheology in the incorporation of new amphiphilic molecules into already formed membranes. Furthermore, ASC_{12} ASC_{14} and ASC_{16} (and not ASC_{10}) are able to penetrate phospholipid monolayers up to a surface pressure of ~ 45–50 mN/m, which is 15–20 mN/m higher than the estimated pressure for lipid bilayers. This strongly suggests that those amphiphilic drugs might be able to integrate into biomembranes.

Finally, the very different pharmacological behaviour for short (ASC_{12}) and long (ASC_{16}) alkyl esters of L-ascorbic acid may be related to the structural alteration of the membrane induced by its incorporation. ASC_{16} promotes the occurrence of LC or/and C domains, when neither ASC_{14} nor ASC_{12} showed this ability, generating a single and fluid phase. In the last years certain relationship of the presence of lipid domains with cellular function has been widely discussed [46]. In this context it is not difficult to relate the possible formation of condensed domains enriched in ASC_{16} in cell membranes and the inflammatory effect observed in tissues exposed to large amount of this drug [8], or the ability of ASC_{12} to mix in a single phase with phospholipids with a mild tissue

irritation when used for drug permeation enhancer [5]. Taking into account the different pharmacological potential of each ASC_n compound, we hypothesize that this may be strongly related to their surface properties and their ability to interact with lipid membranes.

Acknowledgments

This work was supported by the Consejo Nacional de Investigaciones Científicas y Técnicas (CONICET), Agencia Nacional de Promoción Científica y Tecnológica (ANPCyT), and the General Secretary of Science and Technology of Universidad Nacional de Córdoba (SECyT–UNC), Argentina. At present, M.M. is a doctoral student at Instituto de Investigaciones Biológicas y Tecnológicas (IIByT), CONICET–UNC, Depto. de Química, FCEFyN. M.M. and M.V. are CONICET fellows and R.V.V. and M.L.F. are Career Investigators of CONICET–UNC.

Appendix A. Supplementary material

Supplementary data associated with this article can be found, in the online version, at http://dx.doi.org/10.1016/j.jcis.2015.07.014.

References

[1] S.D. Palma, R. Manzo, D. Allemandi, L. Fratoni, P. Lo Nostro, Colloid Surf., A 212 (2003) 163.
[2] S.D. Palma, R. Manzo, P. Lo Nostro, D. Allemandi, Int. J. Pharm. 345 (2007) 26–34.
[3] S.D. Palma, R. Manzo, D. Allemandi, L. Fratoni, P. Lo Nostro, Langmuir 18 (2002) 9219–9224.
[4] L. Benedini, S. Antollini, M.L. Fanani, S.D. Palma, P. Messina, P. Schulz, Mol. Membr. Biol. 31 (2014) 85–94.
[5] L.I. Tartara, D.A. Quinteros, V. Saino, D.A. Allemandi, S.D. Palma, J. Ocul. Pharmacol. Ther. 28 (2012) 102–109.
[6] V. Saino, D. Monti, S. Burgalassi, S. Tampucci, S.D. Palma, D. Allemandi, P. Chetoni, Eur. J. Pharm. Biopharm. 76 (2010) 443–449.
[7] N. Kharrat, I. Aissa, M. Sghaier, M. Bouaziz, M. Sellami, D. Laouini, Y. Gargouri, J. Agric. Food Chem. 62 (2014) 9118–9127.
[8] M.F. Sanchez Vallecillo, G.V. Ullio Gamboa, S.D. Palma, M.F. Harman, A.L. Chiodetti, G. Moron, D.A. Allemandi, M.C. Pistoresi-Palencia, B.A. Maletto, Biomaterials 35 (2014) 2529–2542.
[9] P. Lo Nostro, G. Capuzzi, P. Pinelli, N. Mulinacci, A. Romani, F.F. Vincieri, Colloid Surf., A 167 (2000) 83–93.
[10] H.A. Dabbagh, F. Azami, Food Chem. 164 (2014) 355–362.
[11] L. Benedini, E.P. Schulz, P. Messina, S.D. Palma, D. Allemandi, P. Schulz, Colloids Surf., A 375 (2011) 178–185.
[12] G. Capuzzi, P. Lo Nostro, K. Kulkarni, J.E. Fernandez, F.F. Vincieri, Langmuir 12 (1996) 5413–5418.
[13] G. Capuzzi, K. Kulkarni, J.E. Fernandez, F.F. Vincieri, P. Lo Nostro, J. Colloid Interface Sci. 186 (1997) 271–279.
[14] G. Capuzzi, P. Lo Nostro, K. Kulkarni, J.E. Fernandez, Langmuir 12 (1996) 3957–3963.
[15] M. Mottola, N. Wilke, L. Benedini, R.G. Oliveira, M.L. Fanani, Biochim. Biophys. Acta 1828 (2013) 2496–2505.
[16] L. Benedini, M.L. Fanani, B. Maggio, N. Wilke, P. Messina, S. Palma, P. Schulz, Langmuir 27 (2011) 10914–10919.
[17] G.L. Gaines, Insoluble Monolayers at Liquid–Gas Interfaces, Interscience Publishers, New York, 1966.
[18] U. Kohler, H.H. Mantsch, H.L. Casal, Can. J. Chem. 66 (1987) 983–988.
[19] T. Heimburg, Thermal Biophysics of Membranes, Wiley-VCH Verlag GmbH & Co. KGaA, Berlin, 2007.
[20] J.M. Smaby, M.M. Momsen, H.L. Brockman, R.E. Brown, Biophys. J. 73 (1997) 1492–1505.
[21] B. Maggio, F.A. Cumar, R. Caputto, Biochem. J. 171 (1978) 559–565.
[22] C. Lheveder, J. Meunier, S. Henon, in: A. Baszkin, W. Norde (Eds.), Brewster Angle Microscopy, Physical Chemistry of Biological Interfaces, Marcel Dekker Inc., NY, 2000.
[23] D. Vollhardt, Curr. Opin. Colloid Interface Sci. 19 (2014) 183–197.
[24] X. Chen, H.C. Allen, J. Phys. Chem. A 113 (2009) 12655–12662.
[25] S. Berger, Tetrahedron 33 (1977) 1587–1589.
[26] A.M. Fracaroli, A.M. Granados, R.H. de Rossi, J. Org. Chem. 74 (2009) 2114–2119.
[27] R.D. Falcone, N.M. Correa, M.A. Biasutti, J.J. Silber, Langmuir 16 (2000) 3070–3076.
[28] O.F. Silva, N.M. Correa, J.J. Silber, R.H. Rossi, M.A. Ferna, Langmuir 30 (2014) 3354–3362.
[29] X.M. Li, J.M. Smaby, M.M. Momsen, H.L. Brockman, R.E. Brown, Biophys. J. 78 (2000) 1921–1931.
[30] F. Dupuy, M.L. Fanani, B. Maggio, Langmuir 27 (2011) 3783–3791.
[31] J.N. Israelachvili, Aggregation of amphiphilic molecules into micelles, bilayers and biological membranes, Intermol. Surf. Forces (1991) 366–389.
[32] D.A. Peñalva, N. Wilke, B. Maggio, M.I. Aveldano, M.L. Fanani, Langmuir 30 (2014) 4385–4395.
[33] T.J. Matshaya, A.E. Lanterna, A.M. Granados, R.W. Krause, B. Maggio, R.V. Vico, Langmuir 30 (2014) 5888–5896.
[34] G.A. Borioli, B. Maggio, Langmuir 22 (2006) 1775–1781.
[35] E.J. Grasso, R.G. Oliveira, B. Maggio, Colloids Surf., B 115 (2014) 219–228.
[36] R.V. Vico, O.F. Silva, R.H. de Rossi, B. Maggio, Langmuir 24 (2008) 7867–7874.
[37] R.V. Vico, R.H. de Rossi, B. Maggio, Langmuir 26 (2010) 8407–8413.
[38] M.F. Vega, B. Maggio, N. Wilke, Chem. Phys. Lipids 165 (2012) 232–237.
[39] M.L. Longo, C.D. Blanchette, Biochim. Biophys. Acta 1798 (2010) 1357–1367.
[40] R.M. Weis, H.M. McConnell, Nature 310 (1984) 47–49.
[41] P. Kruger, M. Losche, Phys. Rev. E. Stat. Phys. Plasmas. Fluids Relat. Interdiscip. Top. 62 (2000) 7031–7043.
[42] L. Benedini, S.S. Antollini, M.L. Fanani, S. Palma, P. Messina, P. Schulz, Mol. Membr. Biol. 31 (2014) 85–94.
[43] D. Vollhardt, V.B. Fainerman, Adv. Colloid Interface Sci. 154 (2010) 1–19.
[44] D. Marsh, Biochim. Biophys. Acta 1286 (1996) 183–223.
[45] R.A. Demel, W.S. Geurts van Kessel, R.F. Zwaal, B. Roelofsen, L.L. van Deenen, Biochim. Biophys. Acta 406 (1975) 97–107.
[46] M. Edidin, Annu. Rev. Biophys. Biomol. Struct. 32 (2003) 257–283.